



1 Rapid Communication: Middle Pleistocene Transition as a

2 Phenomenon of Orbitally Enabled Sensitivity to Initial

3 Values

5 Mikhail Y. Verbitsky^{1,2} and Anne Willem Omta³

¹Gen5 Group, LLC, Newton, MA, USA

²UCLouvain, Earth and Life Institute, Louvain-la-Neuve, Belgium

³Department of Earth, Environmental, and Planetary Sciences, Case Western Reserve University, Cleveland, OH, USA

Correspondence: Mikhaïl Verbitsky (verbitskys@gmail.com)

Abstract. The Middle Pleistocene Transition (MPT), i.e., the “fast” transition from \sim 41- to \sim 100-kyr rhythmicity that occurred about 1 Myr ago, remains one of the most intriguing phenomena of the past climate. The cause of this period shift is generally thought to be a change within the Earth System, since the orbital insolation forcing does not change its pattern through the MPT. Using a dynamical model rooted in ocean chemistry, we advance three novel concepts here: (a) the MPT could be a dominant-period relaxation process that is strongly dependent on the initial state of the system, (b) this sensitivity to the initial state is enabled by the orbital forcing, and (c) depending on the amplitude of the orbital forcing and initial values, the MPT could have been not just of the 40 – 80 kyr type, as we observe in the available data, but also of a 20 – 40, 80 – 100, 40 – 120, or even 80 – 40 kyr type.

1. Introduction

Around 1 Myr ago, the dominant period of the glacial-interglacial cycles shifted from ~41 to ~100 kyr (see Fig. 1).

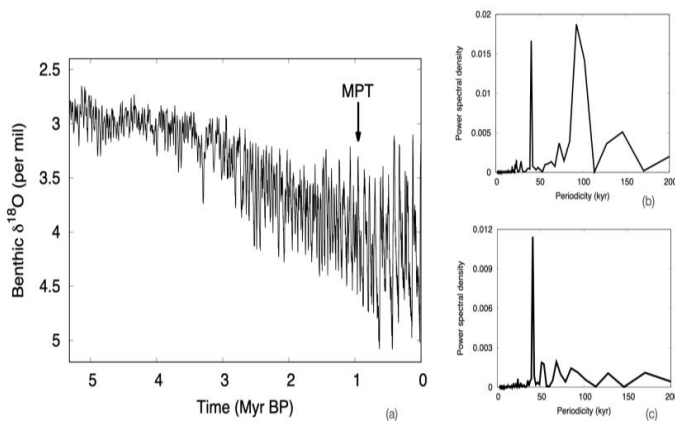


Figure 1. (a) The Mid-Pleistocene Transition (MPT) is visible as a shift in the period and amplitude of the glacial-interglacial cycles around 1 Myr ago in the benthic foraminifera $\delta^{18}\text{O}$ record (Lisiecki and Raymo, 2005), which is a proxy for global ice volume (time goes forward to the right). (b) $\delta^{18}\text{O}$ frequency spectrum between 1 Myr ago and the present (post MPT); note the dominant peak at \sim 100 kyr. (c) $\delta^{18}\text{O}$ frequency spectrum between 2 Myr and 1 Myr ago (pre MPT); note the dominant peak at \sim 40 kyr. This figure was reproduced from Shackleton et al. (2023).



32 The disambiguation of this change in glacial rhythmicity, i.e., the Middle Pleistocene Transition, or
33 MPT hereafter, has been a challenge for the scientific community throughout the last few decades (e.g.,
34 Saltzman and Verbitsky, 1993; Clark and Pollard, 1998; Tziperman et al., 2006; Crucifix, 2013; Mitsui
35 and Aihara, 2014; Paillard, 2015; Ashwin and Ditlevsen, 2015; Verbitsky et al., 2018; Willeit et al., 2019;
36 Riechers et al., 2022; Shackleton et al., 2023; Carrillo et al., 2025; Scherrenberg et al., 2025; Pérez-
37 Montero et al., 2025). Since the orbital insulation forcing does not change its pattern through the MPT,
38 several proposed hypotheses included slow changes in governing parameters *internal to the Earth System*.
39 These may define intensities of positive (e.g., variations in carbon dioxide concentration, Saltzman and
40 Verbitsky, 1993) or negative (e.g., regolith erosion, Clark and Pollard, 1998) system feedbacks or a
41 combination of positive and negative feedbacks (e.g., the interplay of ice-sheet temperature vertical
42 advection and the geothermal heat flux, Verbitsky and Crucifix, 2021). The importance of the orbital
43 forcing in generating the pre-MPT ~41 kyr cycles and post-MPT ~100 kyr cycles has widely been
44 acknowledged. In particular, it has been suggested that orbital cycles either directly drive these cycles
45 (Raymo et al., 2006; Bintanja and Van de Wal, 2008; Tzedakis et al., 2017) or synchronize auto-
46 oscillations of the Earth's climate (Rial et al., 2013; Nyman and Ditlevsen, 2019; Shackleton et al., 2023).
47 However, the orbital forcing has not been considered to play a role in the origin of the MPT.

48 Recently, it has been proposed (Verbitsky and Volobuev, 2024) that the orbital forcing may play a
49 bigger role and can also change the dynamical properties of the Earth's climate system. For example, it
50 may change the vertical advection of mass and temperature in ice sheets and make their dynamics
51 sensitive to initial values. Is ice physics unique in this sense? To answer this question, in this paper we
52 will consider the calcifier-alkalinity (C-A) model that describes entirely different physics, focusing on the
53 interactions between a population of calcifying organisms and ocean alkalinity (Omta et al., 2013).
54 Previously, it has been shown that:

55 (a) The C-A system relaxes slowly to its asymptotic state, i.e., it has a long memory of its initial
56 conditions (Omta et al., 2013);
57 (b) The asymptotic state of the orbitally forced C-A system depends on its initial conditions (Omta et
58 al., 2016).

59 We will demonstrate here that the relaxation of the dominant period of the orbitally forced C-A
60 system from its initial value to the asymptotic value can include a sharp transition similar to the MPT. We
61 will also perform a scaling analysis of the C-A model and demonstrate that the asymptotic dominant
62 periods are defined by conglomerate similarity parameters combining the amplitude of the orbital forcing
63 and the initial values. In other words, *the orbital forcing enables the dominant-period sensitivity to initial
64 values*.

65

66 2. Ocean calcifier-alkalinity model

67

68 The C-A model was first formulated by Omta et al. (2013) and focuses on the throughput of alkalinity
69 through the World's oceans. The alkalinity is a measure for the buffering capacity of seawater that
70 controls its capacity for carbon storage through the carbonate equilibrium (Broecker and Peng, 1982;
71 Zeebe and Wolf-Gladrow, 2001; Williams and Follows, 2011). Alkalinity is continuously transported into
72 the oceans as a consequence of rock weathering on the continents. When alkalinity is added to the ocean,
73 the solubility of CO_2 increases leading to an uptake of carbon from the atmosphere into the ocean.
74 Removal of alkalinity from the water (through incorporation of calcium carbonate into the shells of
75 calcifying organisms and subsequent sedimentation) leads to a lower CO_2 solubility and thus outgassing
76 of carbon from the ocean into the atmosphere. The C-A model assumes that alkalinity A (mM eq) enters
77 the ocean at a constant rate I_0 (mM eq yr^{-1}). Alkalinity is taken up by a population of calcifying
78 organisms C (mM eq) growing with rate constant k ((mM eq) $^{-1}$ yr^{-1}) and sedimenting out at rate M (yr^{-1}).
79 Altogether, the model equations are:

80



$$81 \quad \frac{dA}{dt} = I_0 - kAC \quad (1)$$

$$83 \quad \frac{dc}{dt} = kAC - MC \quad (2)$$

85 with t the time (yr). Since there exists observational evidence of variations in calcifier productivity
 86 correlated with Milankovitch cycles (Beaufort et al., 1997; Herbert, 1997), we include a periodic forcing
 87 term in the calcifier growth parameter k :

$$89 \quad k = k_0 \left(1 + \alpha \cos \left(\frac{2\pi t}{T} \right) \right) \quad (3)$$

90 As in Omta et al. (2016) and Shackleton et al. (2023), k_0 is the average value of k , α is the non-
 91 dimensional forcing amplitude, and T (yr) is the forcing period.

92 Simulations with the C-A model are performed in Julia version 1.11.2. As in Shackleton et al.
 93 (2023), we use the KenCarp58 solver (Rackauckas and Nie, 2017) with a tolerance of 10^{-16} (code is
 94 available on GitHub).

3. Results and Discussion

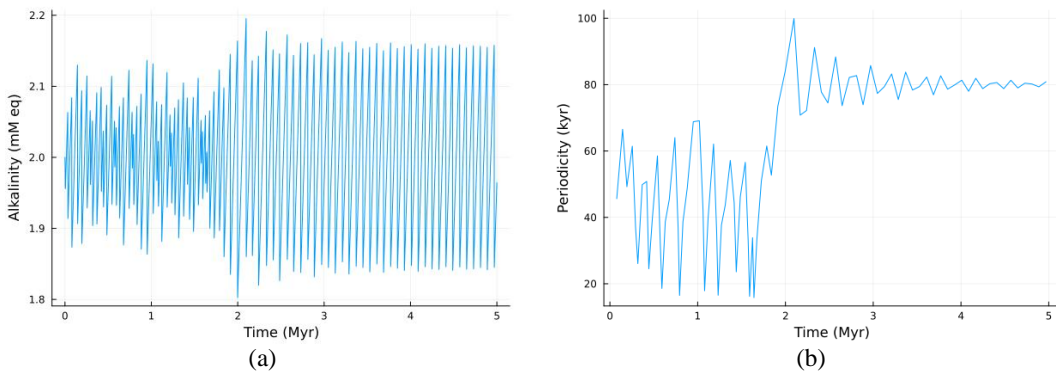


Figure 2. C-A system under orbital forcing ($A(0) = 2.0$ mM eq, $C(0) = 4 * 10^{-5}$ mM eq, $\alpha = 0.012$, $T = 40$ kyr): (a) alkalinity, (b) dominant period as a function of time.

The C-A system (1) – (3) produces sawtooth-shaped cycles in alkalinity, with the alkalinity rising slowly and declining steeply. This corresponds to CO_2 decreasing slowly and increasing rapidly, consistent with the ice-core record (Lüthi et al., 2008). In Fig. 2, a simulation with initial conditions $A(0) = 2.0 \text{ mM eq}$, $C(0) = 4 * 10^{-5} \text{ mM eq}$, forcing strength $\alpha = 0.012$, forcing period $T = 40 \text{ kyr}$, and reference values for other parameters (Omta et al., 2016) is shown. The dominant period initially evolves around the forcing period of 40 kyr, then sharply increases (MPT-like) to about 80 kyr (twice the forcing period) and stabilizes at this level. This period shift occurs through a different mechanism than in earlier studies using the C-A model, where period shifts involved noise (Omta et al., 2016) or a positive feedback (Shackleton et al., 2023) to “kick” the system from one dominant period to another one. Here no such kick is imposed: the period shift rather emerges as part of the transient dynamics of the system, as it relaxes from its initial towards its asymptotic state. For the first $\sim 1.7 \text{ Myr}$ of the simulation, there appears



113 to be an approximate but not exact frequency lock, from which the system has difficulty escaping. Once
114 the system is out of this approximate frequency lock, its period increases relatively rapidly until it reaches
115 another multiple of the forcing period where the system becomes locked again.

116 In the following, we analyze how the “pre-MPT” and “post-MPT” periods may depend on the
117 system parameters. In particular, we formulate a scaling law (Section 3.1) that we then investigate in
118 more detail through simulations (Section 3.2).

119

120 **3.1 Scaling laws**

121

122 The C-A system of equations (1) – (3) contains seven governing parameters, including the initial
123 conditions. Both the mean initial “pre-MPT” and the asymptotic “post-MPT” periods have to be functions
124 of these seven parameters. Thus, we can write:

125

126
$$P = \varphi(I_0, k_0, \alpha, T, M, A(0), C(0)) \quad (4)$$

127

128 with P the asymptotic “post-MPT” period. If we take I_0, k_0 as parameters with independent dimensions,
129 then according to the π -theorem (Buckingham, 1914):

130

131
$$\frac{P}{\tau} = \Phi \left[\alpha, \frac{T}{\tau}, M\tau, \frac{A(0)}{F}, \frac{C(0)}{F} \right] \quad (5)$$

132

133 Here $\tau = (k_0 I_0)^{-1/2}$, $F = \left(\frac{I_0}{k_0}\right)^{1/2}$.

134 Suppose $T, k_0, I_0, M, C(0)$ are constant; then the adimensional period P is a function of two similarity
135 parameters: the orbital forcing amplitude α and the adimensional initial value $\frac{A(0)}{F}$.

136

137
$$\frac{P}{\tau} = \Phi \left[\alpha, \frac{A(0)}{F} \right] \quad (6)$$

138

139 Using similar reasoning, we can write for the “pre-MPT” period P_0 :

140

141
$$\frac{P_0}{\tau} = \Psi \left[\alpha, \frac{A(0)}{F} \right] \quad (7)$$

142

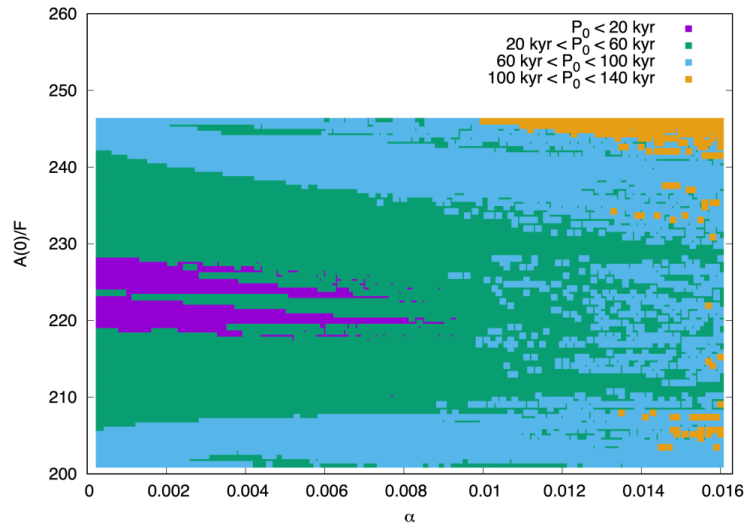
143 **3.2 Scaling law simulations**

144

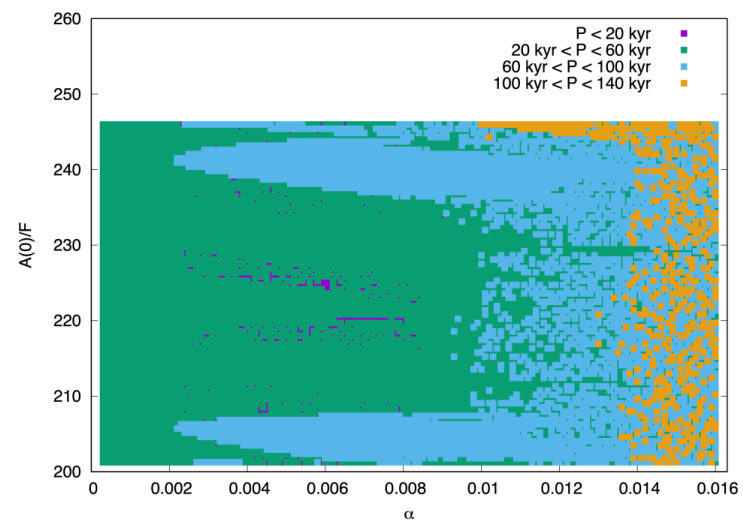
145 To investigate the scaling laws (6, 7), we perform a suite of 10-Myr simulations in which we vary α and
146 $\frac{A(0)}{F}$. The average period during the first 1 Myr (P_0 or “pre-MPT”) and the last 1 Myr (P or “post-MPT”)
147 as a function of α and $\frac{A(0)}{F}$ are presented in Figs. 3a and 3b, respectively.



(a)



(b)



148

149 **Figure 3.** (a) Pre-MPT periods P_0 (average of first 1 Myr of 10-Myr simulations), and (b) post-MPT
150 periods P (average of last 1 Myr of 10-Myr simulations). Each dot represents one simulation.



151

152 From Fig. 3, it can be observed that:

153

154 (a) P_0 and P depend on α and $\frac{A(0)}{F}$ in different manners. Most obviously, $P_0 < 20$ kyr in a significant
155 fraction of the simulations whereas $P > 20$ kyr in almost every simulation. Furthermore, $P > 100$ kyr
156 occurs in many more simulations than $P_0 > 100$ kyr. These differences imply that a period shift
157 emerges in a significant fraction of the simulations.

158 (b) When $\alpha \rightarrow 0$, the “post-MPT” period P becomes independent of the initial value $A(0)$ (Fig. 3b). It
159 means that that the similarity parameters $\alpha, \frac{A(0)}{F}$ in the C-A system (1) – (3) collide into one
160 conglomerate similarity parameter $\alpha^x \left[\frac{A(0)}{F} \right]^y$ (parameters x and y should be determined through
161 simulations). It provides us with the final form of the scaling law for the “post-MPT” period:

162

$$163 \frac{P}{\tau} = \Phi \left\{ \alpha^x \left[\frac{A(0)}{F} \right]^y \right\} \quad (8)$$

164

165

166 The scaling law eq. (8) implies that the *orbital forcing affects the dynamical properties of the C-A physics*
167 *enabling the sensitivity of post-MPT periods to initial values.*

168 (c) When α increases, the sensitivity of the dominant post-MPT period to the initial conditions $\frac{d(\frac{P}{\tau})}{d(\frac{A(0)}{F})}$
169 also increases. Specifically, when $\alpha < 0.002$, as we have already noted, $\frac{P}{\tau}$ is not sensitive to initial
170 values. When $0.002 < \alpha < 0.01$, it takes $\Delta \left(\frac{A(0)}{F} \right) \sim 10$ to obtain a different post-MPT period.
171 Orbital forcing with $0.01 < \alpha < 0.014$ reduces the critical value of initial values changes to
172 $\Delta \left(\frac{A(0)}{F} \right) \sim 1$, and finally for $\alpha > 0.014$ changes as small as $\Delta \left(\frac{A(0)}{F} \right) \sim 0.1$ lead to different
173 post-MPT periods.

174 (d) Depending on $\alpha^x \left[\frac{A(0)}{F} \right]^y$, the MPT transition could have been not just 40 – 80 kyr type, but also 20 –
175 40, 80 – 100, 40 – 120, or even 80 – 40 kyr type (compare Figs. 3a and 3b).

176

177 4. Conclusions

178

179 The history of climate has been given to us as a single time series. For many years, perhaps
180 somewhat naively, significant efforts have been applied to reproduce this time-series under a unique
181 combination of the governing parameters and thus presumably to explain the history (Peacock et al., 2006;
182 Abe-Ouchi et al., 2013; Willeit et al., 2019). The fundamental fact that the dominant-period trajectory is
183 governed by a conglomerate similarity parameter $\alpha^x \left[\frac{A(0)}{F} \right]^y$ (demonstrating a property of incomplete
184 similarity as defined by Barenblatt, 2003) tells us that the MPT could have been produced under very
185 different combinations of the intensity of orbital forcing and initial values. Most intriguingly, the
186 conglomerate similarity parameter $\alpha^x \left[\frac{A(0)}{F} \right]^y$ also tells us that such an “intimate” terrestrial property as
187 the sensitivity of alkalinity-calcination system to initial values manifests itself only under orbital forcing,
188 and thus *MPT exhibits a remarkable physical phenomenon of orbitally enabled sensitivity to initial
189 values.*

190



191

192 **Competing interests:** The authors declare that they have no conflict of interest.

193 **Author contributions:** MYV conceived the research, AWO performed simulations and discovered the
194 MPT-like periodicity relaxation, MYV performed scaling analysis and discovered orbitally enabled
195 sensitivity to initial values. The authors jointly wrote and edited the paper.

196 **References**

197 Abe-Ouchi, A., Saito, F., Kawamura, K., Raymo, M. E., Okuno, J., Takahashi, K., and Blatter, H.:
198 Insolation-driven 100,000-year glacial cycles and hysteresis of ice-sheet volume, *Nature*, 500, 190–193,
199 <https://doi.org/10.1038/nature12374>, 2013.

200 Ashwin, P. and Ditlevsen, P. D.: The middle Pleistocene transition as a generic bifurcation on a slow
201 manifold, *Clim. Dynam.*, 45, 2683–2695, <https://doi.org/10.1007/s00382-015-2501-9>, 2015.

202 Barenblatt, G. I.: *Scaling*, Cambridge University Press, Cambridge, UK, ISBN 0 521 53394 5, 2003.

203 Beaufort, L., Lancelot, Y., Camberlin, P., Cayre, O., Vincent, E., Bassinot, F., and Labeyrie, L.:
204 Insolation cycles as a major control of Equatorial Indian Ocean primary production, *Science*, 278, 1451–
205 1454, 1997.

206 Bintanja, R. and Van de Wal, R. S. W.: North American ice-sheet dynamics and the onset of 100,000-year
207 glacial cycles, *Nature*, 454, 869–872, <https://doi.org/10.1038/nature07158>, 2008.

208 Broecker, W. S. and Peng, T. H.: *Tracers in the Sea*, Lamont-Doherty Geological Observatory, Palisades,
209 NY, USA, ISBN 9780961751104, 1982.

210 Buckingham, E.: On physically similar systems; illustrations of the use of dimensional equations, *Phys.
211 Rev.*, 4, 345–376, 1914.

212 Carrillo, J., Mann, M.E., Marinov, I., Christiansen, S.A., Willeit, M. and Ganopolski, A.: Sensitivity of
213 simulations of Plio–Pleistocene climate with the CLIMBER-2 Earth System Model to details of the global
214 carbon cycle. *Proceedings of the National Academy of Sciences*, 122(23), p.e2427236122, 2025.

215 Clark, P. U. and Pollard, D.: Origin of the middle Pleistocene transition by ice sheet erosion of regolith,
216 *Paleoceanography*, 13, 1–9, 1998.

217 Crucifix, M.: Why could ice ages be unpredictable?, *Clim. Past*, 9, 2253–2267,
218 <https://doi.org/10.5194/cp-9-2253-2013>, 2013.

219 Herbert, T.: A long marine history of carbon cycle modulation by orbital-climatic changes, *Proc. Natl.
220 Acad. Sci.*, 94, 8362–8369, 1997.

221 Lisiecki, L. E. and Raymo, M. E.: A Pliocene-Pleistocene stack of 57 globally distributed benthic $\delta^{18}\text{O}$
222 records, *Paleoceanography*, 20, PA1003, <https://doi.org/10.1029/2004PA001071>, 2005.



223 Lüthi, D., Le Floch, M., Bereiter, B., Blunier, T., Barnola, J. M., Siegenthaler, U., Raynaud, D., Jouzel, J.,
224 Fischer, H., Kawamura, K., and Stocker, T.F.: High-resolution carbon dioxide concentration record
225 650,000-800,000 years before present, *Nature*, 453, 379–382, <https://doi.org/10.1038/nature06949>, 2008.

226 Mitsui, T. and Aihara, K.: Dynamics between order and chaos in conceptual models of glacial cycles,
227 *Clim. Dynam.*, 42, 3087–3099, 2014.

228 Nyman, K. H. M., and Ditlevsen, P. D.: The Middle Pleistocene Transition by frequency locking and
229 slow ramping of internal period, *Clim. Dynam.*, 53, 3023–3038, <https://doi.org/10.1007/s00382-019-04679-3>, 2019.

230 Omata, A.W., Van Voorn, G.A.K., Rickaby, R.E.M., Follows, M.J.: On the potential role of marine
231 calcifiers in glacial–interglacial dynamics, *Global Biogeochem. Cycles*, 27, 692–704,
232 <https://doi.org/10.1002/gbc.20060C>, 2013.

233 Omata, A.W., Kooi, B. W., Van Voorn, G.A.K., Rickaby, R.E.M., Follows, M.J.: Inherent characteristics
234 of sawtooth cycles can explain different glacial periodicities, *Clim. Dynam.*, 46, 557–569,
235 <https://doi.org/10.1007/s00382-015-2598-x>, 2016.

236 Paillard, D.: Quaternary glaciations: from observations to theories, *Quaternary Sci. Rev.*, 107, 11–24,
237 <https://doi.org/10.1016/j.quascirev.2014.10.002>, 2015.

238 Peacock, S., Lane, E., and Restrepo, J. M.: A possible sequence of events for the generalized glacial-
239 interglacial cycle, *Global Biogeochem. Cycles*, 20, GB2010, <https://doi.org/10.1029/2005GB002448>,
240 2006.

241 Pérez-Montero, S., Alvarez-Solas, J., Swierczek-Jereczek, J., Moreno-Parada, D., Robinson, A., and
242 Montoya, M.: Understanding the Mid-Pleistocene transition with a simple physical model, EGUsphere
243 [preprint], <https://doi.org/10.5194/egusphere-2025-2467>, 2025.

244 Rackauckas, C. and Nie, Q.: Differential equations.jl - A performant and feature-rich ecosystem for
245 solving differential equations in Julia, *J. Open Res. Softw.*, 5, 15, <https://doi.org/10.5334/jors.151>, 2017.

246 Raymo, M. E., Lisiecki, L. E., and Nisancioglu, K. H.: Plio-Pleistocene Ice Volume, Antarctic Climate,
247 and the Global $\delta^{18}\text{O}$ Record, *Science*, 313, 492–495, <https://doi.org/10.1126/science.1123296>, 2006.

248 Rial, J. A., Oh, J., and Reischmann, E.: Synchronization of the climate system to eccentricity forcing and
249 the 100,000-year problem, *Nature Geosci.*, 6, 289–293, <https://doi.org/10.1038/ngeo1756>, 2013.

250 Riechers, K., Mitsui, T., Boers, N., and Ghil, M.: Orbital insolation variations, intrinsic climate
251 variability, and Quaternary glaciations, *Clim. Past*, 18, 863–893, <https://doi.org/10.5194/cp-18-863-2022>,
252 2022.

253 Saltzman, B. and Verbitsky, M. Y.: Multiple instabilities and modes of glacial rhythmicity in the Plio-
254 Pleistocene: a general theory of late Cenozoic climatic change, *Clim. Dynam.*, 9, 1–15, 1993.



256 Scherrenberg, M. D. W., Berends, C. J., and Van de Wal, R. S. W.: CO₂ and summer insolation as drivers
257 for the Mid-Pleistocene Transition, *Clim. Past*, 21, 1061–1077, <https://doi.org/10.5194/cp-21-1061-2025>,
258 2025.

259 Shackleton, J. D., Follows, M. J., Thomas P. J., and Omta, A. W.: The Mid-Pleistocene Transition: a
260 delayed response to an increasing positive feedback? *Clim. Dynam.*, 60, 4083–4098,
261 <https://doi.org/10.1007/s00382-022-06544-2>, 2023.

262 Tzedakis, P. C., Crucifix, M., Mitsui, T., and Wolff, E. W.: A simple rule to determine which insolation
263 cycles lead to interglacials, *Nature*, 542, 427–432, <https://doi.org/10.1038/nature21364>, 2017.

264 Tziperman, E., Raymo, M. E., Huybers, P., and Wunsch, C.: Consequences of pacing the Pleistocene
265 100 kyr ice ages by nonlinear phase locking to Milankovitch forcing, *Paleoceanography*, 21, PA4206,
266 <https://doi.org/10.1029/2005PA001241>, 2006.

267 Verbitsky, M. Y. and Crucifix, M.: ESD Ideas: The Peclet number is a cornerstone of the orbital and
268 millennial Pleistocene variability, *Earth Syst. Dynam.*, 12, 63–67, <https://doi.org/10.5194/esd-12-63-2021>, 2021.

270 Verbitsky, M. Y. and Volobuev, D.: Milankovitch Theory “as an Initial Value Problem”, EGUsphere
271 [preprint], <https://doi.org/10.5194/egusphere-2024-1255>, 2024.

272 Verbitsky, M. Y., Crucifix, M., and Volobuev, D. M.: A theory of Pleistocene glacial rhythmicity, *Earth*
273 *Syst. Dynam.*, 9, 1025–1043, <https://doi.org/10.5194/esd-9-1025-2018>, 2018.

274 Willeit, M., Ganopolski, A., Calov, A., and Brovkin, V.: Mid-Pleistocene transition in glacial cycles
275 explained by declining CO₂ and regolith removal, *Science Advances* 5, 4,
276 <https://www.science.org/doi/10.1126/sciadv.aav7337>, 2019.

277

278 Williams, R.G. and Follows, M.J.: Ocean dynamics and the carbon cycle, Cambridge University Press,
279 Cambridge, UK, ISBN 9780521843690, 2011.

280

281 Zeebe, R. E. and Wolf-Gladrow, D.A.: CO₂ in seawater: Equilibrium, kinetics, isotopes, Elsevier,
282 Amsterdam, Netherlands, ISBN 9780444509468, 2001.